ELSEVIER

Polymer 42 (2001) 3077–3086

polymer

www.elsevier.nl/locate/polymer

Kinetics and modeling of free radical polymerization of *N*-vinylformamide

L. Gu, S. Zhu*, A.N. Hrymak, R.H. Pelton

Department of Chemical Engineering, McMaster University, Hamilton, Ont., Canada L8S 4L7

Received 19 May 2000; received in revised form 24 August 2000; accepted 24 August 2000

Abstract

Free radical polymerization kinetics of *N*-vinylformamide was investigated in bulk and in aqueous solution. The molecular weight development with *N*-vinylformamide conversions was measured using a gel permeation chromatography (GPC). The bulk process showed a typical "gel effect" from the beginning of the polymerization. The molecular weight increased steadily at low conversion and leveled off at high conversion. In the solution polymerization, the "gel effect" became less pronounce with decreasing monomer concentration. When the monomer concentration was less than 40 wt%, no auto-acceleration was observed from the time-conversion curves. The $k_p/k_t^{1/2}$ values of the polymerization system were determined using the initial rates of bulk polymerization and the number average molecular weight data at 50, 60 and 70°C. A kinetic model based on free volume theory was proposed to describe the polymerization kinetics and molecular weight development. The model agreed with the time-conversion and conversion-average molecular weight data. © 2001 Elsevier Science Ltd. All rights reserved.

Keywords: *N*-vinylformamide; Polymerization kinetics; Molecular weight distribution

1. Introduction

N-vinylformamide (NVF), an isomer of acrylamide, was developed as a precursor for the production of polyvinylamine by the hydrolysis of poly(*N*-vinylformamide) (PNVF) [1]. The monomer has low toxicity and high reactivity for homo and copolymerization. Free radical polymerization is the most convenient method to produce PNVF although other methods include cationic [2] and anionic polymerization [3].

Industrial interest in PNVF and its derivatives is due to their potential applications in technologies such as wastewater treatment [4] and papermaking [5–9], and to their use as a possible replacement for acrylamide polymers. However, a description of the fundamental polymerization kinetics has not appeared in the literature. Schmidt and coworkers [10] presented a DSC study of NVF bulk polymerization. The $k_p/k_t^{1/2}$ values were estimated to be 1.70 and 2.03 l/(mol s)$^{0.5}$ at 70 and 80°C, respectively. Their study focused more on the evaluation of the thermal measurement techniques employed than the polymerization itself.

In this paper, we compose the results of an experimental investigation and model simulation for both the bulk and aqueous solution polymerization of NVF. The effects of temperature, monomer and initiator concentrations on the polymerization kinetics and molecular weight development are described. A free volume theory was incorporated in the model to describe the kinetic behavior and molecular weight development throughout the polymerization.

2. Experimental

NVF monomer (Aldrich Inc.) was distilled under vacuum at 70°C and stored at −15°C before polymerization. The free radical initiator, 2,2′-azoisobutyronitirle (AIBN) and 2,2′-azobis(2-methylpropionamidine)dihydrochloride (AIBA) (Aldrich Inc.) were recrystallized twice before use. Millipore purified water was used for the aqueous solution polymerization.

A given mixture of NVF and AIBN (NVF, AIBA and water in the case of solution polymerization) was charged in a set of glass ampoules, which were subject to three freeze-to-thaw cycles. After degassing, the ampoules were immersed into a bath with circulating water at the polymerization temperature. Ampoules were taken out at different time intervals and frozen quenched. The reactant mixture was dissolved in water and the polymer content precipitated in methanol. All samples were dried under vacuum at room

* Corresponding author. Tel.: +1-905-525-9140; fax: +1-905-521-1350.
E-mail address: zhuship@mcmaster.ca (S. Zhu).

0032-3861/01/$ - see front matter © 2001 Elsevier Science Ltd. All rights reserved.
PII: S0032-3861(00)00654-6

Nomenclature

α	volume expansion coefficient
ε	volume contraction factor
ϕ	volume fraction
λ_i	the ith moment of living polymer chains
μ_i	the ith moment of dead polymer chains
B	volume ratio of solvent and initial monomer, $B = V_s/V_0$
C_{fp}	chain transfer constant to polymer
C_m	chain transfer constant to monomer
d_m	monomer density (g/cm^3)
d_p	polymer density (g/cm^3)
f	initiation efficiency
$[I]$	initiator concentration (mol/l)
k_p	propagation rate constant (l/(mol s)
k_t	termination rate constant (l/(mol s)
[M]	monomer concentration (mol/l)
M_0	initial mass of monomer (g)
$\bar{M}_n$	number average molecular weight
$\bar{M}_w$	weight average molecular weight
$[P]$	total dead polymer chain concentration (mol/l)
$[P_n]$	concentration of dead polymer chains with n repeat units (mol/l)
$[R^{\cdot}]$	total free radical concentration (mol/l)
$[R_n^{\cdot}]$	concentration of free radical chains with n repeat units (mol/l)
R_p	rate of polymerization (mol/(l s))
V_0	initial monomer volume (l)
V_f	free volume fraction of polymerization system
V_s	solvent volume (l)
W_p	mass of polymer (g)
x	polymerization conversion

Subscripts

0	initial condition or at zero conversion
c	with chemical control
d	with diffusion control
g	glass temperature
m	monomer
p	polymer or propagation
s	solvent
t	termination

temperature for 48 h. The polymerization conversion x, was calculated using:

$$x = \frac{W_p}{M_0} \tag{1}$$

where W_p is the mass of polymer, and M_0 is the initial charge of monomer.

The molecular weight was measured using a Waters aqueous gel permeation chromatography (GPC), 2690 separation module and 2410 refractive index detector equipped with three Waters Ultrahydrogel™ Linear GPC columns ($\phi 7.8 \times 300$ mm). The column temperature was maintained at 30°C. The mobile phase was 0.05 N $NaNO_3$ water solution subjected to filtration (0.4 μm). Polyacrylamide (PAM) standard molecular weight samples (broad standards) ranging from 12,000 to 6 million were purchased from Polysciences Inc. A universal calibration was used with $K = 0.000543$ and $\alpha = 0.715$ for the PNVF samples [11].

3. Experimental results

3.1. Bulk polymerization kinetics

Figs. 1–3 show the bulk polymerization kinetics at 0.006, 0.012 and 0.030 mol/l AIBN concentrations, each with three temperature levels, 50, 60 and 70°C. All the

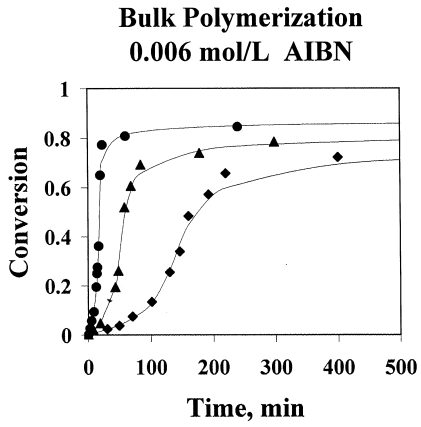

Fig. 1. Kinetics of NVF bulk polymerization, [I] = 0.006 mol/l, ◆ 50, ▲ 60, and ● 70°C, — model.

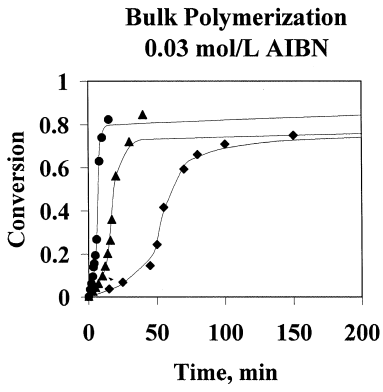

Fig. 3. Kinetics of NVF bulk polymerization, [I] = 0.030 mol/l, ◆ 50, ▲ 60, and ● 70°C, — model.

time-conversion curves displayed an auto-acceleration in the rate ("gel effect") from the start of the polymerization. The final conversion increased with increasing polymerization temperature. The glass transition temperature of PNVF was approximately 122°C measured by DSC at a 10°C/min heating rate. The bulk polymerization yielded a glassy, colorless, transparent monomer–polymer mixture. No visible phase separation was observed throughout the polymerization.

Both the number-average molecular weight ($\bar{M}_n$) (Figs. 4–6) and weight average molecular weight ($\bar{M}_w$) (Figs. 7–9) of the NVF bulk polymerization increased with conversion from the start of the polymerization. The $\bar{M}_w$ of the samples ranged from several hundred thousand to approximately 5 million. These values are comparable to the free radical polymerization of acrylamide.

Under certain experimental conditions, the system gelled. At 50°C and all three initiator concentration levels, and at 60°C with 0.006 mol/l AIBN concentration, gel was found at the final stage of the polymerization. The gelation was accompanied by a reduction in molecular weight of the sol content shown in Figs. 7–9 (at >60% conversion). The gelation mechanism may be due to chain transfer to polymer followed by termination by recombination. This mechanism can also explain the trend of the molecular weight increase with conversion from the start of the polymerization. For those samples without gel, $\bar{M}_w$ tended to level off at high conversions. All low conversion (<5%) samples had a polydispersity index (PDI, $\bar{M}_w/\bar{M}_n$) greater than two.

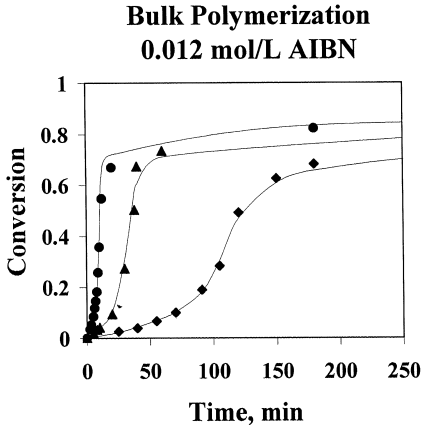

Fig. 2. Kinetics of NVF bulk polymerization, [I] = 0.012 mol/l, ◆ 50, ▲ 60, and ● 70°C, — model.

3.2. Aqueous solution polymerization kinetics

Fig. 10 shows the solution polymerization kinetics at 50, 60 and 70°C with the monomer concentration of 40 wt% (5.63 mol/l) and initiator (AIBA) concentration of 1.47×10^{-3} mol/l. Fig. 11 shows the kinetics at 2.94×10^{-3} mol/l AIBA. These polymerization systems proceeded to near completion. Fig. 12 shows the data at 60°C with different monomer concentrations, 100 wt% (bulk), 40, 20, and 10 wt%. The initiator concentration was 2.94×10^{-3} mol/l based on the total initial reaction volume. The dilution of monomer displayed a trend of increasing final conversion and decreasing of auto-acceleration.

Similar to the bulk system, the high monomer concentration solution polymerization exhibited an increasing trend in $\bar{M}_n$ and $\bar{M}_w$ with conversion from the very beginning of the

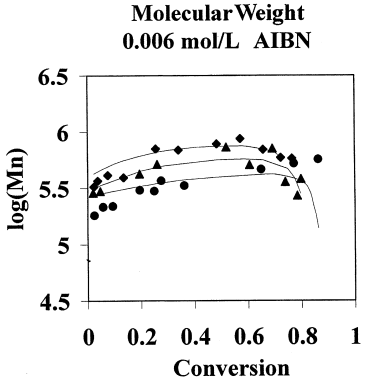

Fig. 4. Development of $\bar{M}_n$ with conversion in bulk polymerization, [I] = 0.006 mol/l, ◆ 50, ▲ 60, and, ● 70°C, — model.

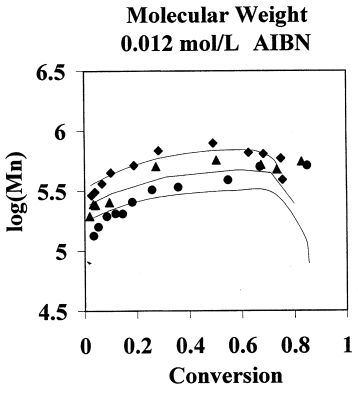

Fig. 5. Development of $\bar{M}_n$ with conversion in bulk polymerization, [I] = 0.012 mol/l, ◆ 50, ▲ 60, and, ● 70°C, — model.

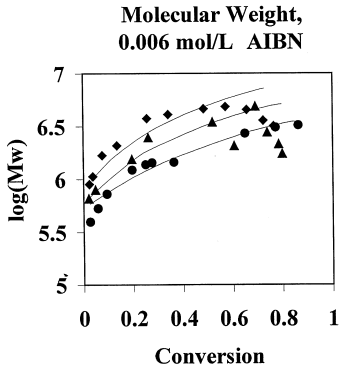

Fig. 7. Development of $\bar{M}_w$ with conversion in bulk polymerization, [I] = 0.006 mol/l, ◆ 50, ▲ 60, and, ● 70°C, — model.

polymerization (see Figs. 13–18). At 20 wt% [M] and 60°C, $\bar{M}_n$ and $\bar{M}_w$ leveled off after 10% conversion. At 10 wt% [M], the $\bar{M}_n$ and $\bar{M}_w$ developed a maximum and dropped thereafter (Figs. 15 and 18). These can be attributed to higher radical mobility in lower viscosity solutions. The solution polymerization at 50°C experienced gelation at about 70% conversion for both 1.47 and 2.94 mmol/l initiator concentrations (Figs. 13 and 16). No gel was observed under other solution polymerization conditions.

4. Model development

4.1. Isothermal polymerization kinetics

In free radical polymerization, the formation of NVF polymer chains consists of three kinetic stages, initiation, propagation and termination. The main side reactions are chain transfers to monomer and polymer. Table 1 summarizes these elementary reactions and their rate expressions. The chain transfers to monomer and to polymer are two major side reactions.

The long chain hypothesis is applied so that the monomers consumed during initiation and chain transfer reactions were ignored. The long chain radical concentrations are defined in population balance equations. The balance equations for radicals and dead polymer chains are summarized in Table 2 for an isothermal batch polymerization process.

During the polymerization, volume contraction was significant and must be considered. The volume contraction factor is defined as

$$\varepsilon = (d_p - d_m)/d_p \tag{2}$$

where d_p and d_m are the densities of polymer and monomer. The volume of reaction mixture at conversion x is therefore

$$V = V_0(1 - \varepsilon x) + V_s = V_0(1 - \varepsilon x + B) \tag{3}$$

where V_0 is the initial monomer volume. V_s is the solvent volume and $B = V_s/V_0$. The method of moments is used to simplify the infinite number of balance equations. The ith moments of living and dead polymer chains are defined by

$$\lambda_i = \sum_{n=1}^{\infty} n^i [R_n^{\cdot}] \tag{4}$$

$$\mu_i = \sum_{n=1}^{\infty} n^i [P_n] \tag{5}$$

However, a higher order dead polymer moment μ_3 is

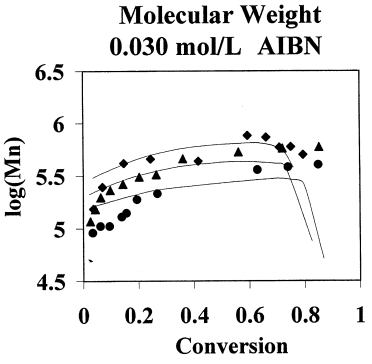

Fig. 6. Development of $\bar{M}_n$ with conversion in bulk polymerization, [I] = 0.030 mol/l, ◆ 50, ▲ 60, and, ● 70°C, — model.

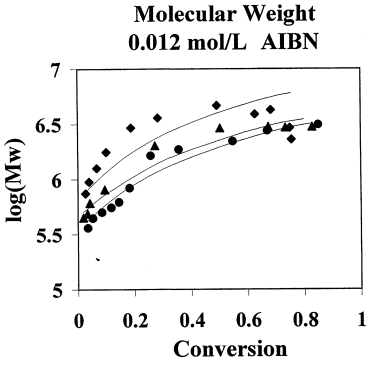

Fig. 8. Development of $\bar{M}_w$ with conversion in bulk polymerization, [I] = 0.012 mol/l, ◆ 50, ▲ 60, and, ● 70°C, — model.

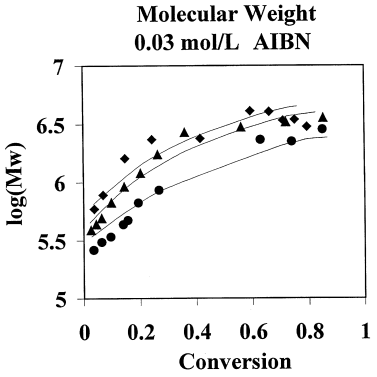

Fig. 9. Development of $\bar{M}_w$ with conversion in bulk polymerization, [I] = 0.030 mol/l, ◆ 50, ▲ 60, and, ● 70°C, — model.

involved in calculating λ_2 because of the chain transfer to polymer mechanism. This is solved by applying quasi steady state to radical population, i.e. $d\lambda_i/dt = 0$. The model can be further simplified by calculating the sum of the radical and dead polymer chain moments, $(\mu_i + \lambda_i)$, instead of individual ones. The final sets of rate equations of the model to be solved are listed in Table 3.

The cumulative number-average ($\bar{M}_n$) and weight-average ($\bar{M}_w$) molecular weights can thus be found by

$$\bar{M}_n = \frac{\lambda_1 + \mu_1}{\lambda_0 + \mu_0} \tag{6}$$

$$\bar{M}_w = \frac{\lambda_2 + \mu_2}{\lambda_1 + \mu_1} \tag{7}$$

4.2. Diffusion-controlled propagation and termination

Both the rates of propagation and termination are subject to diffusion control due to the limited mobility of long chain

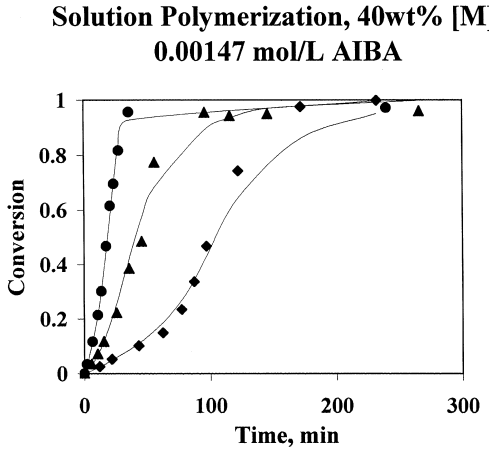

Fig. 10. Kinetics of NVF aqueous solution polymerization, [I] = 1.47×10^{-3} mol/l, [M] = 5.63 mol/l or 40 wt%, ◆ 50, ▲ 60, and ● 70°C, — model.

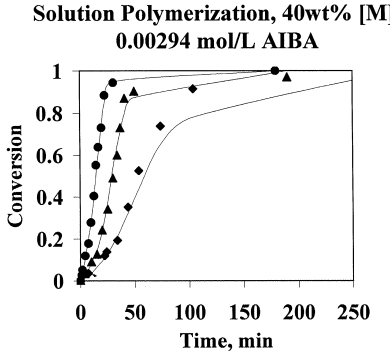

Fig. 11. Kinetics of NVF aqueous solution polymerization, [I] = 2.94×10^{-3} mol/l, [M] = 5.63 mol/l or 40 wt%, ◆ 50, ▲ 60, and ● 70°C, — model.

radicals caused by viscosity increase and/or chain entanglement (i.e. the "gel effect"). The onset of the diffusion-controlled termination occurs much earlier than that of propagation because the termination involves diffusion of two long chains.

Two different attempts on modeling the gel effect of free radical polymerizations have been made. One is that of O'Driscoll [12,13] and Tirrell [14] based on the ideas of polymer chain entanglement. The other is based on the free volume theory [15], which is used in this paper. Modeling diffusion-controlled polymerization process using the free volume theory is a semi-empirical approach by its nature. This method has been applied and tested over the whole range of conversion for various polymerization systems. The Chiu–Carratt–Soong (CCS) model [16] and Marten–Hamielec (MH) model [17,18] are two representative models. The MH model suggested that the "gel effect" would not take place until a 'critical' point is reached. This leads to a discontinuous feature in the model and 'artificial onset' free volume fraction values for the diffusion-controlled termination and propagation. In comparison, the CCS model proposed that the effective kinetic constants (both propagation and termination) are the sum of the

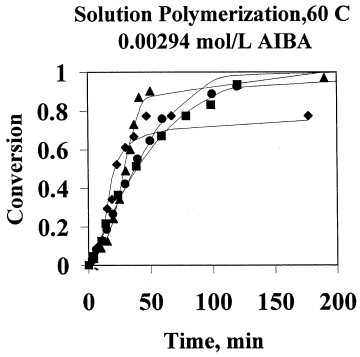

Fig. 12. Kinetics of NVF aqueous solution polymerization at 60°C with varying monomer concentration, [I] = 2.94×10^{-3} mol/l, ◆ bulk, ▲ 5.63 mol/l or 40 wt%, ● 2.82 mol/l or 20 wt%, and ■ 1.41 mol/l or 10 wt%, — model.

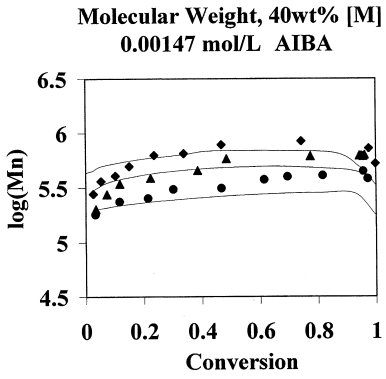

Fig. 13. Development of $\bar{M}_n$ with conversion in solution polymerization, [I] = 1.47×10^{-3} mol/l, [M] = 5.63 mol/l or 40 wt%, ◆ 50, ▲ 60, and ● 70°C, — model.

inverse of diffusion-controlled constant and that of a chemical constant. In this case, both propagation and termination are considered to be diffusion controlled at the beginning of the polymerization:

$$\frac{1}{k_{\mathrm{eff},i}} = \frac{1}{k_{\mathrm{chem},i}} + \frac{1}{k_{\mathrm{diff},i}} \quad i = \text{propagation or termination} \tag{8}$$

Applying Eq. (8) to propagation and termination yields.

$$\frac{1}{k_{\mathrm{p}}} = \frac{1}{k_{\mathrm{p,c}}} + \frac{1}{k_{\mathrm{p,d}}} \tag{9}$$

$$\frac{1}{k_{\mathrm{t}}} = \frac{1}{k_{\mathrm{t,c}}} + \frac{1}{k_{\mathrm{t,d}}} \tag{10}$$

where the diffusion-controlled constants were defined as

$$k_{\mathrm{p,d}} = k^0_{\mathrm{p,d}} \exp\left(-\frac{a_{\mathrm{p}}}{V_{\mathrm{f}}}\right) \tag{11}$$

$$k_{\mathrm{t,d}} = k^0_{\mathrm{t,d}} \exp\left(-\frac{a_{\mathrm{t}}}{V_{\mathrm{f}}}\right) \tag{12}$$

where V_{f} is the free volume fraction of the reaction mixture.

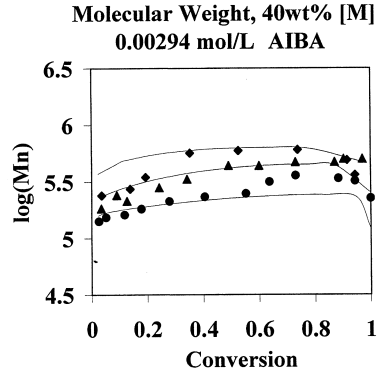

Fig. 14. Development of $\bar{M}_{\mathrm{n}}$ with conversion in solution polymerization, [M] = 5.63 mol/l, [M] = 5.63 mol/l or 40 wt%, ◆ 50, ▲ 60, and ● 70°C, — model.

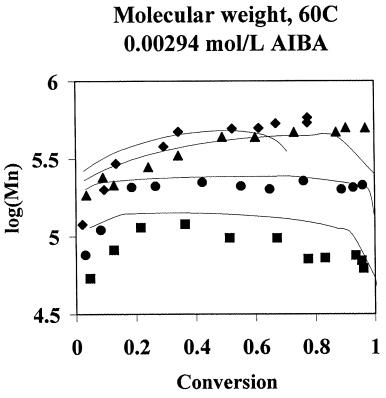

Fig. 15. Development of $\bar{M}_{\mathrm{n}}$ with conversion in solution polymerization, 60°C with varying monomer concentration, [I] = 2.94×10^{-3} mol/l, ◆ bulk, ▲ 5.63 mol/l or 40 wt%, ● 2.82 mol/l or 20 wt%, and ■ 1.41 mol/l or 10 wt%, — model.

$k^0_{\mathrm{p,d}}$ and $k^0_{\mathrm{t,d}}$ are two pseudo-kinetic constants related to the diffusion nature in the polymerization system [19]. The parameter a_{t} in Eq. (12) is further defined as a linear function of the conversion, i.e. $a_{\mathrm{t}} = a^0_{\mathrm{t}} + a^1_{\mathrm{t}} x$. The model equations of the diffusion controlled kinetic constants are summarized in Table 4.

4.3. Simulation results

Before the model can be used to simulate the polymerization process, several physical properties of the initiator, monomer and polymer must be obtained or estimated.

(1) Initial combined rate constant ($k_{\mathrm{p,c}}/k^{0.5}_{\mathrm{t,c}}$) and chain transfer to monomer, $C_{\mathrm{m}}(= k_{\mathrm{fm}}/k_{\mathrm{p}})$.

According to Eq. (13), the combined rate constant $k_{\mathrm{p,c}}/k^{0.5}_{\mathrm{t,c}}$ and chain transfer constant C_{m} can be estimated from the initial polymerization rate and the $\bar{M}_{\mathrm{n}}$ data:

$$\frac{1}{\bar{M}_{\mathrm{n}}} = \frac{k_{\mathrm{t,c}} R_{\mathrm{p}}}{(k_{\mathrm{p,c}}[\mathrm{M}])^2} + C_{\mathrm{m}} \tag{13}$$

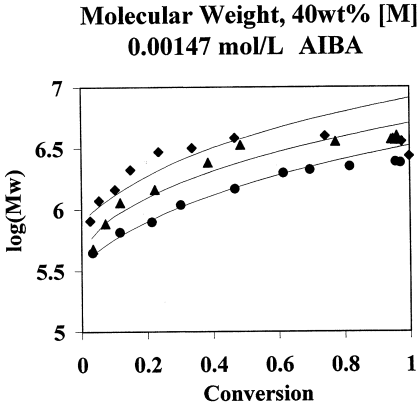

Fig. 16. Development of $\bar{M}_{\mathrm{w}}$ with conversion in solution polymerization, [I] = 1.47×10^{-3} mol/l, [M] = 5.63 mol/l or 40 wt%, ◆ 50, ▲ 60, and ● 70°C, — model.

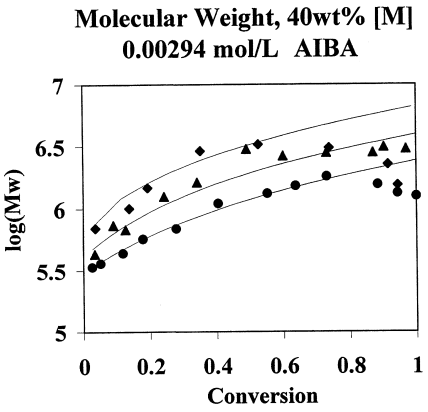

Fig. 17. Development of $\bar{M}_w$ with conversion in solution polymerization, [I] = 2.94×10^{-3} mol/l, [M] = 5.63 mol/l or 40 wt%, ◆ 50, ▲ 60, and ● 70°C, — model.

To obtain the polymerization rate, the data summarized in Table 5 are used. The values of $\Delta x/\Delta t$ were taken as equal to dx/dt. Therefore

$$R_p = [M]\frac{dx}{dt} \approx [M]\frac{\Delta x}{\Delta t} \quad (14)$$

The right hand side of Eq. (13) is plotted against $R_p/[M]^2$ data. The slopes of the least squares linear fitting give the inverse of $k_{p,c}/k_{t,c}^{0.5}$ and the intercept, C_m. The data were summarized in Table 6. Within the scope of this investigation, $k_{p,c}$ and $k_{t,c}$ cannot be estimated separately.

(2) Glass transition temperature of the monomer (T_{gm}) and polymer (T_{gp}).

The glass transition of NVF monomer can be estimated using Fedors' correlation [20], $T_{gm} = -112$°C. T_{gp} is obtained using DSC, $T_{gp} = 122$°C.

(3) Thermal expansion factors of the monomer (α_m) and polymer (α_p).

The thermal expansion factors, α_m and α_p are used in the present model to calculate the free volume fraction during

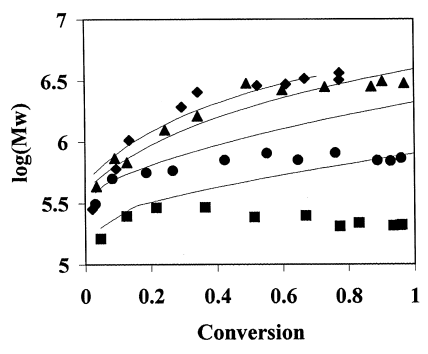

Fig. 18. Development of $\bar{M}_w$ with conversion in solution polymerization, 60°C with varying monomer concentration, [I] = 2.94×10^{-3} mol/l, ◆ bulk, ▲ 5.63 mol/l or 40 wt%, ● 2.82 mol/l or 20 wt%, and ■ 1.41 mol/l or 10 wt%, — model.

Table 1
Kinetics of NVF bulk free radical polymerization

Initiation	$I \rightarrow 2R^{\cdot}$	$R_i = 2fk_d[I]$
Propagation	$R_n^{\cdot} + M \rightarrow R_{n+1}^{\cdot}$	$R_p = k_p[R_n^{\cdot}][M]$
	$R_n^{\cdot} + R_m^{\cdot} \rightarrow P_{n+m}$ (recombination)	$R_{tc} = k_{tc}[R_n^{\cdot}][R_m^{\cdot}]$
	Or $P_n + P_m$ (disproportionation)	$R_{td} = k_{td}[R_n^{\cdot}][R_m^{\cdot}]$
Chain transfer	$R_n^{\cdot} + M \rightarrow R_1^{\cdot} + P_n$ (to monomer)	$R_{fm} = k_{fm}[M][R_n^{\cdot}]$
	$R_n^{\cdot} + P_m \rightarrow R_m^{\cdot} + P_n$ (to polymer)	$R_{fp} = k_{fp}[P][R_n^{\cdot}]$

Table 2
Population balance equations

$1/Vd([M]V)/dt = -k_p[M]\sum_1^\infty [R_i^{\cdot}]$
$1/Vd([I]V)/dt = -k_d[I]$
$1/Vd([R_1^{\cdot}]V)/dt = 2fk_d[I] - k_t[R_1^{\cdot}]\sum_1^\infty [R_i^{\cdot}] + k_{fm}[M]\lambda_0$
$1/Vd([R_n^{\cdot}]V)/dt = k_p[M]([R_{n-1}^{\cdot}] - [R_n^{\cdot}]) - k_t[R_n^{\cdot}]\sum_1^\infty [R_i^{\cdot}] - k_{fm}[M][R_n^{\cdot}] - k_{fp}([R_n^{\cdot}]\sum_1^\infty i[P_i] - n[P_n]\sum_1^\infty [R_i^{\cdot}]) \quad n > 2$
$1/Vd([P_n]V)/dt = k_{td}[R_n^{\cdot}]\sum_1^\infty [R_i^{\cdot}] + k_{fm}[M][R_n^{\cdot}] + k_{fp}([R_n^{\cdot}]\sum_1^\infty i[P_i] - n[P_n]\sum_1^\infty [R_i^{\cdot}]) \quad n > 1$

Table 3
Model equations

$dV/dt = -(V_0/(1+B))\varepsilon dx/dt$
$d[I]/dt = -k_d[I] - [I]/VdV/dt$
$dx/dt = k_p(1-x)\lambda_0$
$d\lambda_0/dt = 2fk_d[I] - k_t\lambda_0^2 - \lambda_0/VdV/dt$
$d\lambda_1/dt = 2fk_d[I] - k_t\lambda_0\lambda_1 + k_{fm}[M](\lambda_0 - \lambda_1) + k_p[M]\lambda_0 - k_{fp}(\lambda_1\mu_1 - \lambda_0\mu_2) - \lambda_1/VdV/dt$
$d\lambda_2/dt = 2fk_d[I] - k_t\lambda_0\lambda_2 + k_{fm}[M](\lambda_0 - \lambda_2) + k_p[M](2\lambda_1 + \lambda_0) - k_{fp}(\lambda_2\mu_1 - \lambda_0\mu_3) - \lambda_2/VdV/dt$
$d(\lambda_0 + \mu_0)/dt = d\mu_0/dt = 2fk_d[I] + k_{fm}[M]\lambda_0 - \mu_0/VdV/dt$
$d(\lambda_1 + \mu_1)/dt = d\mu_1/dt = 2fk_d[I] + k_{fm}[M]\lambda_0 + k_p[M]\lambda_0 - \mu_1/VdV/dt$
$d(\lambda_2 + \mu_2)/dt = d\mu_2/dt = 2fk_d[I] + k_{fm}[M]\lambda_0 + k_p[M](2\lambda_1 + \lambda_0) - \mu_2/VdV/dt$

Table 4
Modeling diffusion-controlled kinetic constants

$1/k_p = 1/k_{p,c} + 1/k_{p,d}$
$k_{p,d} = k_{p,d}^0 \exp(-a_p/V_f)$
$V_f = \phi_m V_{fm} + \phi_p V_{fp} + \phi_s V_{fs} = \phi_m[0.025 + \alpha_m(T - T_{gm})] + \phi_p[0.025 + \alpha_p(T - T_{gp})] + \phi_S[0.025 + \alpha_s(T - T_{gs})]$
$a_t = a_t^0 + a_t^0 x$
$a_p = 0.4,\ a_t^0 = 1.0$
$1/k_t = 1/k_{t,c} + 1/k_{t,d}$
$k_{t,d} = k_{t,d}^0 \exp(-a_t/V_f)$

polymerization. The value of α_m was calculated from the reported NVF density data [21].

$$\alpha_m = 9.53 \times 10^{-4} \quad (15)$$

A regression method was used to find the α_p. The free

volume fraction of the PNVF–NVF mixture at the final conversion was taken to be 0.025 [22].

$$V_f = \phi_m[0.025 + \alpha_m(T - T_{gm})] + \phi_p[0.025 + \alpha_p(T - T_{gp})] \quad (16)$$

Given the temperature, the corresponding final conversion (bulk polymerization, Table 5) and α_m, α_p can be obtained by a least squares fit

$$\alpha_p = 7.32 \times 10^{-4} \quad (17)$$

For comparison purposes, the suggested "universal" values [22,23] are 10.0×10^{-4} and 4.8×10^{-4} for α_m and α_p, respectively.

The model calculation and parameter regression was implemented with the MATLAB 5.0 software package. The ordinary differential equation solver was a second order Runge–Kutta method (ODE23S) and the optimizer (FMINS) used a Nelder–Mead type simplex search method. The minimization objective function for fitting the model was defined as

$$\text{obj} = \sum_i \frac{(x_{\text{exp},i} - x_{\text{mod},i})^2}{(x_{\text{exp},i})^2} + \sum_i \frac{(M_{\text{wexp},i} - M_{\text{wmod},i})^2}{(M_{\text{wexp},i})^2} \quad (18)$$

The number-average molecular weight data, $\bar{M}_n$, were not used in fitting, but calculated using the estimated kinetic parameters obtained from the regression.

In the event of gelation, only the conversion data of the samples were included in the objective function. The molecular weights of the sol samples were not included. In the calculation, data for $k_{t,d}$ of acrylamide [24] was used. The parameters to be estimated were $k^0_{p,d}$, $k^0_{t,d}$, C_{fp} ($= k_{fp}/k_p$) and a^1_t. The parameter a_p was set to 0.4 and a^0_t to 1.0 for all the polymerization temperatures and initiator concentrations [15,25].

The rate constants and physical properties used in the model calculation are summarized in Table 7. The regressed parameters are listed in Tables 8 and 9 for bulk and solution polymerization, respectively. The regressed conversion, $\bar{M}_w$ and calculated $\bar{M}_n$ results from the model are plotted as solid lines along with the experimental data points from Figs. 1–18. In general, the model is able to describe the polymerization behavior, both the conversion and the molecular weight sufficiently.

In the bulk polymerization, the model gives a better fit of the time-conversion data than the conversion-$\bar{M}_w$ data. It over-predicts $\bar{M}_n$ at the start of the polymerization and shows a slower increase than the experimental $\bar{M}_n$. The regressed $k^0_{p,d}$ value increases with initiator concentration at each temperature level. The $k^0_{t,d}$ value also increases with initiator concentration with the exception at 60°C, 0.012 mol/l [I] (see Table 8). The values of a^1_t presented in Table 8 do not show a clear pattern over the range of experimental conditions. The C_{fp} values at different initiator levels are similar at the same temperature and increase with polymerization temperature.

In the solution polymerization, the average values of C_{fp} obtained in the regression of the bulk polymerization at 50, 60 and 70°C are used as known constants. The parameters to be fit are thus reduced to $k^0_{p,d}$, $k^0_{t,d}$ and a^1_t and the results are summarized in Table 9.

The model, which does not consider gelation, over-estimates $\bar{M}_w$ at the final stage of polymerization at 50°C where gelation was observed at >70% conversion. The model gives a good agreement to conversion, $\bar{M}_w$ and $\bar{M}_n$ data at monomer concentrations >40%. However, the model is poor in describing the molecular weight data when the

Table 5
Low conversion $\bar{M}_n$ and $\bar{M}_w$ data and the final conversions of bulk polymerization

T (°C)	[I] (mol/l)	Time (min)	Conversion	$\bar{M}_n \times 10^{-3}$	$\bar{M}_w \times 10^{-3}$	PDI	Final conversion
50	0.006	30	0.024	327	897	2.7	0.77
		49	0.037	367	1063	2.9	
	0.012	20	0.027	291	746	2.6	0.76
		35	0.039	310	951	3.1	
	0.030	15	0.037	154	527	3.4	0.79
60	0.006	8	0.020	287	668	2.4	0.80
		19	0.047	296	799	2.7	
	0.012	5	0.019	194	449	2.3	0.83
		8	0.034	245	629	2.5	
	0.030	3	0.026	117	378	3.2	0.85
70	0.006	3	0.026	182	397	2.2	0.86
		5.5	0.058	215	540	2.5	
	0.012	2.5	0.035	133	358	2.7	0.85
		3.5	0.052	159	441	2.8	
	0.030	1.17	0.034	91.2	265	3.2	0.85

Table 6
Combined rate constants, $k_{p,c}/k_{t,c}^{0.5}$ and chain transfer constant, C_m (= k_{fm}/k_p)

T (°C)	$k_{p,c}/k_{t,c}^{0.5}$, l/(mol s)$^{0.5}$	$C_m \times 10^4$
50	0.090	7.33
60	0.143	9.37
70	0.245	18.0

Table 7
Rate constants and physical properties

Property	Value	Reference
f	0.6	
k_d	2.88×10^{15} exp(−15686/t) (S^{-1}) AIBN	Xie [26]
	9.42×10^{14} exp(−14860/t) (s^{-1}), AIBA	Polymer handbook [27]
$k_{t,c}^{0.5}$	9.19×10^4 exp(−741/t) (l/mol/min), acrylamide	Hunkler [24]
d_m	1.01–0.98 (g/cm^3)	Singley [21]
d_p	1.25 (g/cm^3)	Estimated, this research
T_{gm}	−122 (°C)	Calculated from Fedors [20]
T_{gp}	112 (°C)	This research
T_{gs}	−136 (°C)	Fedors [20]
Molecular weight	71, monomer	
	164, AIBN	
	271, AIBA	
α_m	9.53×10^{-4} (°C^{-1})	Calculated from Singley [21]
α_P	7.32×10^{-4} (°C^{-1})	This research
α_s	5.54×10^{-4} (°C^{-1})	Calculated from Perry [28]

Table 8
Simulation results of bulk polymerization

T, (°C)	[I], mol/l	$k_{p,d}^0 \times 10^{-3}$	$k_{t,d}^0 \times 10^{-7}$	$C_{fp} \times 10^3$	a_t^1
50	0.006	0.106	0.255	1.11	3.40
	0.012	0.365	4.05	1.29	3.12
	0.030	0.866	14.4	0.99	3.16
60	0.006	0.389	2.23	1.36	3.39
	0.012	0.966	10.5	1.20	3.51
	0.030	0.987	7.63	1.58	3.53
70	0.006	0.847	2.78	2.51	2.90
	0.012	1.081	4.72	2.60	3.79
	0.030	10.39	134	2.25	2.38

monomer concentrations are 10 and 20 wt% (Fig. 18), in which the experimental $\bar{M}_w$ leveled off or decreased at an early stage (~20% conversion). In order to fit the time-conversion data, the constraint over the $\bar{M}_w$ data was released in the objective function (Eq. 18). The calculated $\bar{M}_w$ and $\bar{M}_n$ data are plotted in Figs. 16 and 18. The model gives a continuously increasing $\bar{M}_w$ results with conversion. The calculated $\bar{M}_n$ results are higher than the experimental values although the trend is matched. This suggests that other factors need to be considered in a dilute aqueous solution polymerization.

The trend of a_t^1 change is more obvious in solution than in bulk. At a monomer concentration of 40 wt%, the value of a_t^1 decreases as the polymerization temperature increases from 50 to 70°C. The a_t^1 also decreases with the monomer dilution from bulk to 10 wt% at 60°C. In the solution polymerization, a long chain radical has a diffusion rate higher than in bulk. In addition, the free volume fraction loss due to monomer conversion is partially offset by the free volume contribution from solvent. This allows a slower decay in the diffusion controlled termination constant, $k_{t,d}$, which is represented by the change in a_t^1.

5. Conclusions

The free radical polymerization of *N*-vinylformamide was examined in bulk and in aqueous solution processes. The bulk polymerization showed a severe "gel effect" from the start of the polymerization. Both the number-average molecular weight, $\bar{M}_n$, and weight-average molecular weight, $\bar{M}_w$, increased continuously from a very low conversion and then plateaued at the final stage of the polymerization. The $k_{p,c}/k_{t,c}^{0.5}$ and C_m values at 50, 60 and 70°C were obtained using the initial conversion and $\bar{M}_n$ data of the bulk polymerization. For the solution polymerization, the "gel effect" was still pronounced at monomer concentrations greater than 40 wt%. The $\bar{M}_n$ and $\bar{M}_w$ displayed the same increasing trend as that in the bulk polymerization. Further dilution of the monomer with solvent effectively eases the "gel effect". No auto-acceleration in time-conversion curves was observed at 10 and 20 wt% monomer concentrations. A

Table 9
Simulation results of aqueous solution polymerization

T (°C)	[M] (wt%)	$C_{fp} \times 10^3$	[I], (mol/l)	$k_{p,d}^0 \times 10^{-3}$	$k_{t,d}^0 \times 10^{-7}$	a_t^1
50	40	1.13	0.00147	1.27	11.7	2.07
			0.0294	0.225	0.357	2.74
60	40	1.38	0.00147	1.98	15.7	2.13
			0.00294	3.80	44.2	1.78
70	40	2.45	0.00147	6.24	47.7	1.40
			0.00294	1.87	6.01	1.42
60	100	1.380	0.00294	1.73	9.65	1.83
	40			3.80	44.2	1.78
	20			0.369	0.141	0.49
	10			0.270	0.051	0.03

semi-empirical model based on a free volume theory was proposed to describe both the bulk and solution polymerizations. The model was able to fit both the time-conversion data and the conversion- $\bar{M}_w$ data satisfactorily.

Acknowledgements

The authors are grateful to the Natural Sciences and Engineering Research Council of Canada (NSERC) for supporting this research. The authors also thank Drs Stephan Drappel and Daniele Boils of Xerox Research Center of Canada for their kind help on the GPC measurement.

References

[1] Stinson S. Chem Engng News 1993;7(36):32.
[2] Spange S, Madl A, Eismann U, Utecht J. Macromol Rapid Commun 1997;18:1075.
[3] Fikentscher R, Kroener M. (BASF). US Patent, 5155270, 1992.
[4] Burkert H, Brunnmuller F et al. (BASF). US Patent, 4444667, 1984.
[5] Monech D, Hartman H et al. (BASF). US Patent, 5262008, 1993.
[6] Auhorn W, Linhart F et al. (BASF) US Patent, 5145559, 1992.
[7] Pfohl S, Kroener M et al. (BASF) US Patent, 4978427, 1989.
[8] Pfohl S, Kroener M et al. (BASF) US Patent, 4880497, 1989.
[9] Pfohl S, Kroener M et al. (BASF) US Patent, 4774285, 1988.
[10] Schimdt C, Hungenberg K, Hubinger W. Chem Ing Technnol 1996;68:953.
[11] Singley EJ, Daniel A, Person D, Beckman EJ. J Polym Sci Part A, Polym Chem 1997;35:2533.
[12] Cardenas J, O'Driscoll KF. J Polym Sci, Polym Chem Ed 1976;14:883.
[13] Cardenas J, O'Driscoll KF. J Polym Sci, Polym Chem Ed 1977;15:1883.
[14] Tulig TJ, Tirrell M. Macromolecules 1981;14:1501.
[15] Fujita H, Kishimoto A, Matsumoto K. Trans Faraday Soc 1960;56:424.
[16] Chiu WY, Carratt GM, Soong DS. Macromolecules 1983;16:348.
[17] Marten FL, Hamielec AE. ACS Symp Ser 1979;104:43.
[18] Marten FL, Hamielec AE. J Appl Polym Sci 1982;27:489.
[19] Soh SK, Sundberg DC. J Polym Sci, Polym Chem Ed 1982;20:1331.
[20] Fedors RF. J Polym Sci, Polym Lett Ed 1979;17:719.
[21] Singley EJ. Development of fluoroether amphiphiles and their applications in heterogeneous polymerization in supercritical carbon dioxide. PhD Dissertation, University of Pittsburgh, 1997, p. 221.
[22] Bueche F. Physical properties of polymers. New York: Interscience, 1962.
[23] Soh SK, Sundberg DC. J Polym Sci, Polym Chem Ed 1984;22:2243.
[24] Hunkeler DJ. Acrylic water soluble polymers. PhD dissertation, McMaster University, 1990.
[25] Fujita H, Kishimoto A. J Chem Phys 1961;34:393.
[26] Xie T. Vinyl chloride polymerization. PhD dissertation, McMaster University, 1990.
[27] Brandrup J, Immergut EH, editors. Polymer handbook. 2nd ed. New York: Wiley, 1975.
[28] Perry RH, Chilton CH, Perry JH, editors. Chemical engineer's handbook. New York: McGraw-Hill, 1975.